

Certified but Fooled! Breaking Certified Defences with Ghost Certificates

Quoc Viet Vo¹, Tashreque M. Haq¹, Paul Montague³, Tamas Abraham³, Ehsan Abbasnejad²,
Damith C. Ranasinghe¹

¹University of Adelaide

²Monash University

³Defence Science and Technology Group

quocviet.vo@adelaide.edu.au, tashreque.mohammed.haq@adelaide.edu.au, paul.montague@defence.gov.au,
tamas.abraham@defence.gov.au, ehsan.abbasnejad@monash.edu, damith.ranasinghe@adelaide.edu.au

Abstract

Certified defenses promise provable robustness guarantees. We study the malicious exploitation of probabilistic certification frameworks to better understand the limits of guarantee provisions. Now, the objective is to not only mislead a classifier, but also manipulate the certification process to generate a robustness guarantee for an adversarial input—*certificate spoofing*. A recent study in ICLR demonstrated that crafting large perturbations can shift inputs far into regions capable of generating a certificate for an incorrect class. Our study investigates if perturbations needed to cause a misclassification and yet coax a certified model into issuing a deceptive, large robustness radius for a target class can still be made *small* and *imperceptible*. We explore the idea of region-focused adversarial examples to craft imperceptible perturbations, spoof certificates and achieve certification radii larger than the source class—*ghost certificates*. Extensive evaluations with the ImageNet demonstrate the ability to effectively bypass state-of-the-art certified defenses such as Densepure. Our work underscores the need to better understand the limits of robustness certification methods.

Introduction

Deep neural networks (DNNs) are vulnerable to adversarial examples—carefully crafted perturbations to manipulate inputs to coerce incorrect model decisions whilst remaining imperceptible to human observers (Biggio et al. 2013; Szegedy et al. 2014; Papernot et al. 2017; Carlini and Wagner 2017b; Madry et al. 2018; Brendel, Rauber, and Bethge 2018). In response, various empirical defenses such as adversarial training and preprocessing inputs are proposed (Dalvi et al. 2004; Papernot et al. 2016; Buckman et al. 2018; Guo et al. 2018; Samangouei, Kabkab, and Chellappa 2018; Shafahi et al. 2019; Wong, Rice, and Kolter 2020; Rebuffi et al. 2021; Doan et al. 2022). But, demonstrating empirical robustness alone does not facilitate reasoning about robustness guarantees, and strong adaptive attacks can bypass defenses (Carlini and Wagner 2017a; Athalye, Carlini, and Wagner 2018; Tramer et al. 2020; Croce and Hein 2020; Wong, Rice, and Kolter 2020). So, certified robustness has emerged to provide provable lower bounds on model accuracy under bounded perturbations.

Copyright © 2026, Association for the Advancement of Artificial Intelligence (www.aaai.org). All rights reserved.

Conceptually, certification methods provide both a *model* for a task to generate a prediction and a *verifier* for generating a certificate guaranteeing an input image is not an adversarial example under a predefined threat model. Existing certification methods in the vision domain predominantly focus on l_2 or l_∞ -bounded threat models, effectively ensuring that all inputs within an ϵ -ball neighbourhood of a given image are consistently classified under the same label. We focus on the probabilistic *Randomized Smoothing* (Cohen, Rosenfeld, and Kolter 2019; Zhang et al. 2019) frameworks offering scalable certification for tasks.

Unlike conventional attacks—eg., PGD (Madry et al. 2018), Wasserstein (Levine and Feizi 2020), and semantic attacks (Shahin Shamsabadi, Sanchez-Matilla, and Cavallo 2020; Bhattacharjee et al. 2020)—we explore the adversarial exploitation of certified models that *both* mislead the classifier and falsely receive robustness certificates. If attackers can generate an adversarial example that remains imperceptible and semantically consistent, while ensuring neighbouring images within a certification radius share an incorrect label—a verifier is fooled with a spoofed certificate (Ghiasi, Shafahi, and Goldstein 2020).

Our Study. Spoofing attacks introduce a new dimension to the adversarial threat landscape by targeting *both* the classification and certification processes. To investigate the assurances provided by certified defences, we introduce a new certificate spoofing mechanism that systematically undermines classification and certification mechanisms.

Our idea is to explore *if* region-based manipulation of inputs to constrain translation in the input-space—a means to preserve input semantics whilst minimizing manipulation—can still shift inputs in the latent-space just far enough to achieve a misclassified label from a model and yet, a *large* radius certificate from a verifier.

To achieve our idea, we construct a malicious objective to induce high-probability of misclassified neighborhoods to yield certified radii—beyond just fooling classifiers.

Contributions and Findings

- We propose a new algorithm for an adversarial attack to spoof robustness certificates. Unlike the prior study’s constrained manipulation of an input image to seek certifiable adversarials, we consider a region-based approach

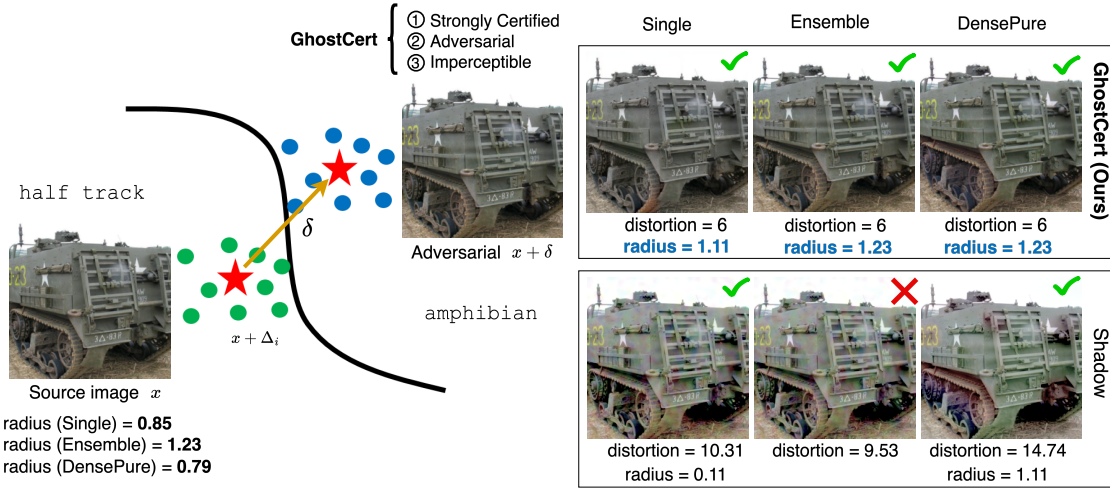


Figure 1: Overview of our attack formulation. For a given source image (*half track*) and certification radii, we show the corresponding adversarial examples created by our attack **GhostCert** and **Shadow** Attack in ICLR (Ghiasi, Shafahi, and Goldstein 2020) against three certified defense methods: Randomized Smoothing (with Resnet50), Smoothed Ensemble, and DensePure (Diffusion based denoiser & Transformer under Randomized Smoothing). **Shadow** fails to generate a spoofed certificate (\times) for Smoothed Ensemble even with a *larger* distortion. **GhostCert** generates more *natural-looking* adversarials across all three defenses while achieving misclassification with: i) higher spoofed certification radii; and ii) significantly lower l_2 norms ($\|\delta\|_2$) compared to the **Shadow** Attack (*Adversarial* and *Imperceptible*). **GhostCert** results also surpass the certification radii of the source image (*Strongly Certified*)—see Fig. 7 for results of a user-study on imperceptibility. **Code:** <https://github.com/ghostcert>

to select areas for perturbation. This enables the perturbation to remain *imperceptible* but more efficacious and evasive because the region selection considers *natural* image boundaries and *salient* regions.

- We provide a rigorous evaluation of our attack algorithm, dubbed **GhostCert**, with the large-scale ImageNet task. To advance the prior evaluation of untargeted attacks, we construct *targetted* attacks, including a significant effort to evaluate with a state-of-the-art certification method based on diffusion models (DensePure).
- We raise awareness of weaknesses in current robustness certification methods & discuss the implications of attacks targeting both classification and certification.

Importantly, while our new exploit demonstrates that existing certification methods can be exploited with stealth, the attack does not invalidate the certificates produced—the assertion made by a certificate that an input is not an adversarial example in the chosen bounded norm is still correct. *Rather, our attack is a cautionary tale.*

Key Takeaways: Safe deployment of systems with certifiably robust models should use certificates as an indicator of label correctness with caution. A strongly certified sample input (with a large certification radius) does not necessarily imply correctness nor that a potential manipulation to spoof a certificate will lead to easily visible evidence. We confirm, even targetted attacks (certification for a target label chosen by an attacker) are possible. But, as expected, are harder. The state-of-the-art denoiser-based method remains the most effective certification method, even when compared to model ensembling under randomised smoothing.

We hope the study helps reveal and deepen understanding of flaws in certified defenses for adversarial robustness.

Related Work

Adversarial attack algorithms can launch powerful attacks like Projected Gradient Descent (PGD) to craft and apply imperceptible perturbations to inputs to mislead or hijack the decision of deep learning models (Szegedy et al. 2014; Papernot et al. 2017; Carlini and Wagner 2017b; Madry et al. 2018; Athalye, Carlini, and Wagner 2018).

The recent **Shadow** Attack in (Ghiasi, Shafahi, and Goldstein 2020) exposes a weakness in a certified defences. The attack generates large perturbations in the input-space to move an image *far* from a class boundary to a region capable of generating a fake certificate with a large radius. The attack augments PGD to constrain semantic changes and perturbations with three penalties: i) to force the perturbation δ to have small total variation to attempt to appear smooth and natural; ii) to limit the perturbation δ by constraining the change in the mean of each color channel; and iii) to promote perturbations that assume similar values in each colour channel to suppress extreme or dramatic colour changes. *We devise a simpler attack and demonstrate that such large perturbations are not necessary to break a certified defence.*

Preliminaries on Scalable Certification

Complete certification methods guarantee finding adversarial examples if they exist, but are limited to small datasets and simple models due to scalability constraints (Weng et al. 2018). Complete methods are typically restricted to specific architectures and struggle with large-scale tasks (Cohen, Rosenfeld, and Kolter 2019; Hayes 2020) like

ImageNet (Deng et al. 2009a). Incomplete approaches, including deterministic (Lyu et al. 2020; Levine and Feizi 2020) and probabilistic methods, can certify the lower bound of model performance under certain ℓ_p norm attacks or abstain from deciding (Li, Xie, and Li 2023). Lecuyer et al. (2019) introduced the incomplete method—*randomized smoothing*—using Gaussian and Laplace noise. This approach offers a general and scalable approach for certification on large scale tasks such as ImageNet. The approach provides a non-trivial probabilistic robustness guarantee. Subsequent studies tightened the bound (Cohen, Rosenfeld, and Kolter 2019) and further improved certified performance by integrating adversarial training (Salman et al. 2019), consistency regularization (Jeong and Shin 2020), and model ensembling (Horváth et al. 2022).

Randomized Smoothing. Consider a classification problem from $\mathbf{x} \in \mathbb{R}^d$ to classes \mathcal{Y} . As introduced in (Cohen, Rosenfeld, and Kolter 2019), randomized smoothing is a method for constructing a new, “smoothed” classifier g from an arbitrary base classifier f . When queried by \mathbf{x} , the smoothed classifier g returns what the base classifier f is most likely to return when \mathbf{x} is perturbed by noise $\mathbf{\epsilon} \sim \mathcal{N}(0, \sigma^2 I)$:

$$g(\mathbf{x}) = \arg \max_{c \in \mathcal{Y}} \mathbb{P}(f(\mathbf{x} + \mathbf{\epsilon}) = c) \quad (1)$$

The noise level σ is a hyperparameter of the smoothed classifier g which controls a robustness/accuracy tradeoff; it does not change with the input \mathbf{x} .

Smoothed Ensemble. Recent work (Horváth et al. 2022) has introduced several advancements to enhance Randomized Smoothing. For a set of k classifiers $\{f^l : \mathbb{R}^d \rightarrow \mathbb{R}^m\}_{l=1}^k$, a soft-ensemble \bar{f} is constructed by averaging the logits $\bar{f}(\mathbf{x}) = \frac{1}{k} \sum_{l=1}^k f^l(\mathbf{x})$, where, $f^l(\mathbf{x})$ are the pre-softmax outputs. With $\mathbf{\epsilon} \sim \mathcal{N}(0, \sigma^2 I)$, the smoothed ensemble can be formulated as follows:

$$g_e(\mathbf{x}) = \arg \max_{c \in \mathcal{Y}} \mathbb{P}(\bar{f}(\mathbf{x} + \mathbf{\epsilon}) = c) \quad (2)$$

Denoised Smoothing. An alternative approach to obtaining a provably robust classifier *without retraining* the underlying model has been proposed through the idea of *denoised smoothing* (Salman et al. 2020). Unlike prior work that primarily focus on training classifiers to withstand Gaussian perturbations—often using Gaussian noise augmentation (Cohen, Rosenfeld, and Kolter 2019) or adversarial training (Salman et al. 2019)—this method leaves the pre-trained classifier unchanged. Building on this idea, several recent methods have explored the use of diffusion-based denoiser such as DiffusionDenoisedSmoothing (DDS) (Carlini et al. 2023), DensePure (Xiao et al. 2023) or DiffSmooth (Zhang et al. 2023). Denoised Smoothing essentially augments the base classifier f with a denoiser $D_\theta : \mathbb{R}^d \rightarrow \mathbb{R}^d$ to form a new base classifier defined as $f \circ D_\theta : \mathbb{R}^d \rightarrow \mathcal{Y}$. Assuming the denoiser D_θ is effective at removing Gaussian noise, this setup is configured to classify well under Gaussian perturbation of its inputs. Formally, with $\mathbf{\epsilon} \sim \mathcal{N}(0, \sigma^2 I)$, this procedure can be defined as follow:

$$g_d(\mathbf{x}) = \arg \max_{c \in \mathcal{Y}} \mathbb{P}[f(D_\theta(\mathbf{x} + \mathbf{\epsilon})) = c] \quad (3)$$

Certifiable Robustness and Abstaining. (Cohen, Rosenfeld, and Kolter 2019) introduces an analytic form of certifiable robustness that provides a formal guarantee for smoothed classifiers. Concretely, the prediction of a smoothed classifier remains unchanged within a bounded ℓ_2 -norm region defined by a certified radius R .

$$R = \frac{\sigma}{2} [\Phi^{-1}(p_A) - \Phi^{-1}(p_B)], \quad (4)$$

where p_A, p_B are the probabilities of the top class c_A and the runner-up class c_B respectively, Φ^{-1} is the inverse Gaussian cumulative distribution function (CDF). Based on Theorem 1 in (Cohen, Rosenfeld, and Kolter 2019), the smoothed classifier $g(\mathbf{x})$ always returns c_A and certified radius $\sigma \Phi^{-1}(p_A)$ if the lower bound of the probability of the top class p_A exceeds 0.5. Otherwise, the smoothed classifier abstains from making a prediction. To prevent an adversary from manipulating the smoothed classifier to abstain at a high rate, a margin μ is introduced as follows:

$$\mathbb{P}(f(\mathbf{x} + \mathbf{\delta} + \mathbf{\epsilon}) = c_A) - \mathbb{P}(f(\mathbf{x} + \mathbf{\delta} + \mathbf{\epsilon}) = c_B) \geq \mu \quad (5)$$

Proposed Method

Threat Model. We consider a white-box threat model for attacks on a target DNN (deep neural network), where adversaries have full access to the model’s architecture, parameters and the noise level used by the smoothed classifier.

Problem Formulation. Given a neural network f , an input \mathbf{x} , and the ground truth label y , we define an adversarial attack as an optimization problem searching for a perturbation $\mathbf{\delta}$ that maximizes the loss function L . The objective is to generate adversarial examples misleading a smoothed classifier while ensuring the perturbation remains imperceptible.

$$\max_{\mathbf{\delta}} \sum_{i=1}^N L(f(\mathbf{x} + \mathbf{\epsilon}_i + \mathbf{\delta}), y) \text{ s.t. } \|\mathbf{\delta}\|_2 \leq \epsilon, \quad (6)$$

where $L(\cdot, \cdot)$ is the loss function, $\mathbf{\delta}$ denotes the adversarial perturbation, ϵ is the perturbation budget, $\mathbf{\epsilon}_i$ represents isotropic Gaussian noise applied to the input, N is the number of noisy samples used to approximate the probability mass in Randomized Smoothing. The formulation of this optimization allows to find an adversarial perturbation $\mathbf{\delta}$ that consistently forces the smoothed model to misclassify the adversarial example $\mathbf{x} + \mathbf{\delta}$.

When the base model is an ensemble of k classifiers $\{f^l : \mathbb{R}^d \rightarrow \mathbb{R}^m\}_{l=1}^k$ and the resulting classifier is \bar{f} , the problem can be formulated as:

$$\max_{\mathbf{\delta}} \sum_{i=1}^N L(\bar{f}(\mathbf{x} + \mathbf{\epsilon}_i + \mathbf{\delta}), y) \text{ s.t. } \|\mathbf{\delta}\|_2 \leq \epsilon, \quad (7)$$

Similarly, when the base model f_θ is subjected to a denoiser D_θ , the new base model becomes $f \circ D_\theta$ and therefore, the problem formulation changes to:

$$\max_{\mathbf{\delta}} \sum_{i=1}^N L(f(D_\theta(\mathbf{x} + \mathbf{\epsilon}_i + \mathbf{\delta})), y) \text{ s.t. } \|\mathbf{\delta}\|_2 \leq \epsilon. \quad (8)$$

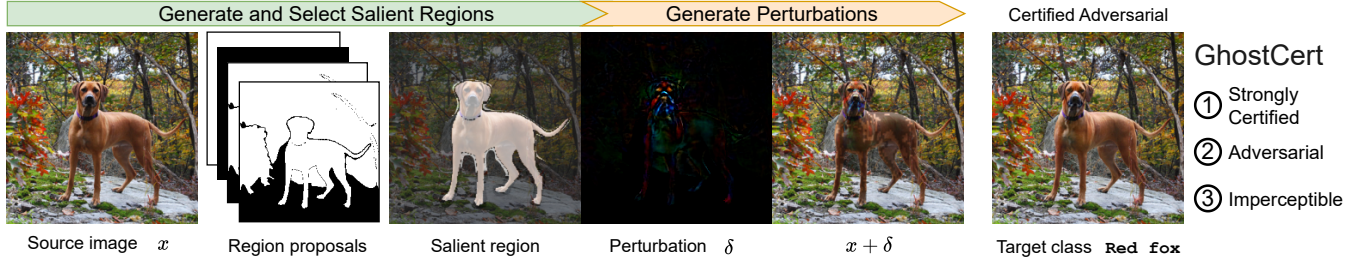


Figure 2: A pictorial illustration of GhostCert. Starting from the source image x with label **Rhodesian ridgeback** and given a target label **Red fox**, region proposal are evaluated to select regions for manipulation considering salient features important for classification decisions. The idea is to preserve semantics whilst minimising distortions. Then, crafting perturbations constrained to the salient regions, δ , yields the adversarial $x + \delta$ misclassified as a **Red fox** while being strongly certified with imperceptible visual differences to the source image x .

Method Intuition

To solve these attack optimization problems, several gradient-based methods such as Fast Gradient Sign Method (FGSM) (Goodfellow, Shlens, and Szegedy 2015), Basic Iterative Method (BIM) (Kurakin, Goodfellow, and Bengio 2017) can be employed. However, Projected Gradient Descent (PGD) (Madry et al. 2018) has emerged and provides superior performance for white-box attacks due to its ability to navigate complex loss surfaces through iterative small steps gradient ascent. Therefore, we adopt PGD in our study to navigate toward the adversarial solution.

While traditional adversarial attacks successfully employ a global perturbation, they have not leveraged saliency information within natural images to enhance the imperceptibility of adversarial perturbation. Recent empirical observations in (Vo, Abbasnejad, and Ranasinghe 2022) demonstrate that, when searching for perturbations to inputs in black-box settings, they tend to concentrate within salient regions of an image, although the attack *does not explicitly target* these regions. This suggests that more effective perturbations could be crafted by manipulating the salient regions.

To identify salient regions with Convolutional-based models, GradCAM (Selvaraju et al. 2017) represents a natural choice due to its widespread adoption in highlighting decision-critical areas. However, GradCAM’s gradient-based saliency maps produce amorphous regions that disregard the natural structural boundaries inherent in images. This results in perturbations producing unnatural artifacts and compromising semantic coherence. To overcome this fundamental limitation, we introduce a new notion—*salient-region masks*—that combines GradCAM’s gradient-driven saliency information with semantic segmentation boundaries derived from the Segment Anything Model (SAM) (Kirillov et al. 2023). Similarly, for transformer-based models, Attention maps provide an alternative to GradCAM, directly revealing which spatial locations the model prioritizes during classification. This integration ensures that perturbations maintain natural-looking boundaries while maintaining focus on salient regions. Our core hypothesis posits that constraining adversarial perturbations to these semantically-coherent salient regions will yield adversarial examples with imperceptibility and preserved semantic meaning.

GhostCert Attack Algorithm

A pictorial illustration of how GhostCert produces the adversarially perturbed image leading to misclassification and certificate spoofing while being visually imperceptible is shown in Figure 2. By using standard image segmentation techniques to generate region proposals, combined with saliency analysis, to select regions defined by natural image boundaries, we aim to generate more natural-looking adversarial examples, that are strongly certified (large spoofed certification radius, often higher or comparable with the source image). Owing to their imperceptibility objective, we refer to these as ghost certificates and dub our method GhostCert.

Generate Salient-Region Mask. Let $\mathcal{S} \in [0, 1]^{H \times W}$ be the saliency map generated by GradCAM or Attention depending on the model under attack, and let $\mathcal{M} = \{M_1, M_2, \dots, M_n\}$ denote the *region proposals*—realised as a set of binary segmentation masks produced by the SAM model, each with area > 300 pixels. Additionally, let U be a binary unmask candidate mask representing pixels not covered by any of the segmentation masks in \mathcal{M} . For each mask $M_i \in \mathcal{M}$, the saliency overlap score is defined as:

$$\text{score}(M_i) = \frac{\sum_{x,y} M_i(x, y) \cdot \mathcal{S}(x, y)}{\sum_{x,y} M_i(x, y) + \sum_{x,y} \mathcal{S}(x, y)}. \quad (9)$$

Similarly, an overlap score for the unmask candidate U is also obtained. Let $\mathcal{T} \subset \mathcal{M} \cup \{U\}$ be the set of top- k masks selected based on the highest scores. The final combined mask—*salient-region mask*— m is then obtained by summing the top- k masks:

$$m = \sum_{M \in \mathcal{T}} M. \quad (10)$$

This salient-region mask m highlights the most salient and semantically meaningful regions, guided by both segmentation and GradCAM/attention-based saliency.

Generate Perturbations. Considering an untargeted attack setting, for every image a batch of noisy images is generated, with each image in the batch subjected to random Gaussian noise of standard deviation σ . The perturbation δ , initially zero, is added to the batch of noisy images, and the following problem is optimized.

$$\begin{aligned} \max_{\delta} \sum_{i=1}^N L(f_{\theta}(x + \Delta_i + \delta \odot m), y) \\ \text{s.t. } \|\delta \odot m\|_2 \leq \epsilon, \end{aligned} \quad (11)$$

where $L(\cdot, \cdot)$ is the loss function. In this work, we use cross-entropy loss. \odot denotes element-wise multiplication, δ is the adversarial perturbation applied to the input, Δ_i represents the random Gaussian noise of standard deviation σ , m is the selective region or mask to perturb, ϵ is the perturbation budget. This selective perturbation, when added to the source image x , while bounded by ϵ produces an adversarial image with visually less perceptible changes. Similarly, when the attack setting is targeted, a target label y_{target} is provided instead of y since the targeted attack aims to fool the model f_{θ} to predict the class label of image x to be y_{target} .

Attack pipeline. We codify the attack in Algorithm 1. Figure 3 shows samples from successful attacks with GhostCert and the prior Shadow Attack.

Algorithm 1 GhostCert

Require: Input image x , ground truth label y , target label y_{target} (if targeted), noise Δ_i , mask m , step size λ , maximum distortion ϵ , attack type (targeted or untargeted)

- 1: Initialize $\delta \leftarrow 0$
- 2: **for** $i = 1$ to N **do**
- 3: **if** attack is targeted **then**
- 4: $g \leftarrow -\nabla_{\delta} L(f_{\theta}(x + \Delta_i + \delta), y_{target})$
- 5: **else**
- 6: $g \leftarrow \nabla_{\delta} L(f_{\theta}(x + \Delta_i + \delta), y)$
- 7: **end if**
- 8: $\delta \leftarrow \delta + \lambda \cdot \frac{g}{\|g\|_2}$ ▷ Gradient ascent/descent step
- 9: $\delta \leftarrow \left(\epsilon \frac{\delta}{\|\delta\|_2}\right) \odot m$ ▷ Projection and mask step
- 10: **end for**
- 11: **return** δ

Experiments and Evaluations

Dataset(s). We used the large-scale ImageNet (Deng et al. 2009b) validation set for experiments as in Shadow Attack. For each base model and σ combination, under Randomized Smoothing, 100 correctly classified images and their certification radii were identified (notably Shadow Attack used 50 samples). This ensures the attacks were carried out considering only images that were correctly certified by the models under Randomized Smoothing. For each set of 100 images, on average, there were 94 to 97 different class labels, suggesting a low bias towards a particular class label.

Defended models and attacks. We employed three certified defenses: i) Randomized Smoothing (RS) with Resnet50 (Single model) (Cohen, Rosenfeld, and Kolter 2019); and ii) Ensemble of three consistency-trained Resnet50 models (Horváth et al. 2022) under RS (with $\sigma = 0.25, 0.5, 1.0$); and iii) diffusion-based denoiser prepended to a BEiT large Patch16 512 transformer under RS (DensePure) (with $\sigma = 0.25, 0.5$) (Xiao et al. 2023). The ensemble was included as part of the defended models because it is well

Table 1: Evaluation protocol summary.

Attack	Pert. Budgets (ϵ)	Defense Methods	Dataset	Perf. Metrics
GhostCert(Ours)	2, 4, 6, 8, 10	Single	ImageNet	ASR
Shadow Attack	N/A	Ensemble		Spoofing Radius
Bounded Shadow Attack ¹	2, 4, 6, 8, 10	DensePure		

Note 1: Our adapted version of Shadow Attack (Ghiasi, Shafahi, and Goldstein 2020) to constrain perturbations.

established that, in terms of certified robustness, an ensemble of consistency-trained models outperforms a single Resnet50, yielding higher certified accuracy under Randomized Smoothing.

To evaluate, three attacks were carried out—GhostCert, current state-of-the-art Shadow Attack, and our modified version Shadow Attack to bound the distortion limit to compare with GhostCert referred to as Shadow Attack (bounded).

Performance Metrics. **Attack Success Rate (ASR).** In the untargeted case, it is the proportion of samples misclassified by the defending model. In the targeted case, it is the proportion of samples classified by the defending model as the target class and assigned a certificate (radius)—if the defence abstains from making a prediction, these were recorded as **Denial of Service (DoS)** attacks. **Spoofing Radius.** This is the certification radius calculated for samples that have been successfully misclassified.

Evaluation Protocol. For both untargeted and targeted settings, ASR and the average Spoofing Radius were reported for evaluation across every defense method. For a targeted attack setting, due to computational constraints, only one target label was chosen for each source image. The target label was determined by sequentially searching for an image with a different label, starting from the following index of the source image. In addition, for targeted attacks, DoS results were reported as well. This process helps eliminate bias in the selection the target label. Table 1 summarizes the evaluation protocols used.

Attacking a (Single) and (Ensemble) Classifier Under Randomised Smoothing

Attack Success Rate (ASR). (**Single**) For both untargeted and targeted attacks, GhostCert consistently achieves significantly higher ASR than both bounded and unbounded shadow attacks across all noise levels ($\sigma = 0.25, 0.5, 1.0$) as demonstrated in Figure 4 and Figure 5.

(**Ensemble**) For untargeted attacks, at $\sigma = 0.25$ GhostCert achieves $\approx 100\%$ ASR while shadow attack and its variant plateau at 40% across different ($\sigma = 0.25, 0.5, 1.0$) as shown in Figure 4. The ensemble defense significantly impacts shadow attack and its variant but has minimal effect on GhostCert’s effectiveness. For targeted attacks, at $\sigma = 0.25$, GhostCert achieves an ASR of over 80% while the shadow variants max out at just over 20% . At higher noise levels ($\sigma = 0.5, 1.0$), while the ASR is not as high across all attacks, GhostCert still produces significantly larger ASR than the shadow attacks as shown in Figure 5.

Overall, the performance gap is most pronounced at higher noise levels, where GhostCert maintains effectiveness while shadow attacks degrade significantly.

Spoofed Radii. (**Single**) For untargeted attacks, GhostCert

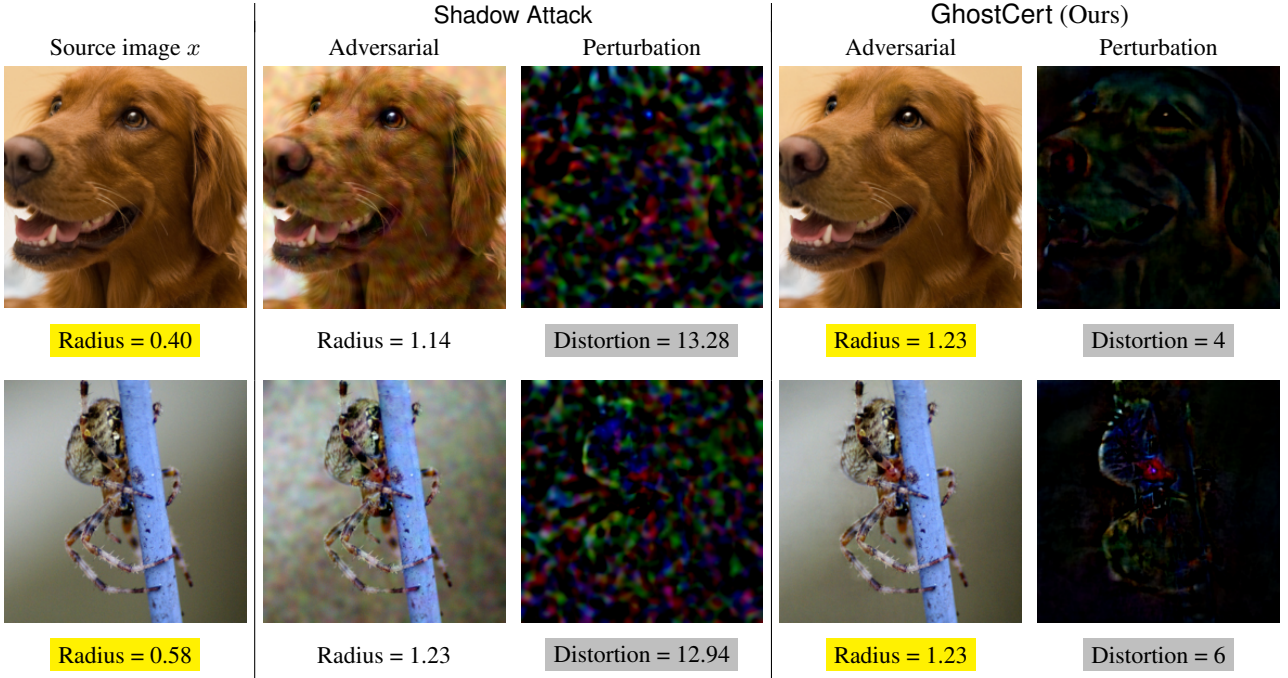


Figure 3: Illustrative examples of successful attacks by GhostCert are presented. For each case, we display the adversarial image and its corresponding perturbation generated by both the Shadow attack and our method, GhostCert. The results clearly show that GhostCert produces strongly certified adversarial examples with perturbations that are more visually imperceptible than those from the Shadow attack, while also achieving higher spoofed certification radii at lower l_2 norms ($\|\delta\|_2$).

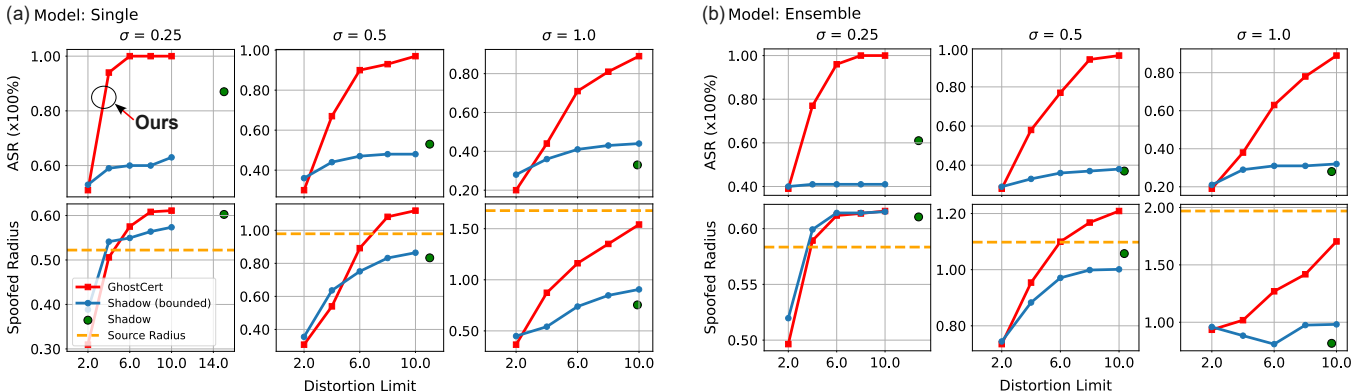


Figure 4: Comparing ASR and spoofed radii for three attacks in *untargeted* settings against (a) single ResNet-50 under Randomized Smoothing (RS) and (b) an ensemble of three consistency ResNet-50 models under RS vs. distortion $\|\delta\|_2$ budgets.

generates substantially larger spoofed radii compared to the shadow baselines, particularly evident at $\sigma = 0.5, 1.0$. Notably, GhostCert's spoofed radii consistently exceed or approach the source certified radius (orange dashed line), indicating effective circumvention of the defense mechanism. For targeted attacks, GhostCert consistently achieves larger spoofed radii than its Shadow Attack counterparts.

(Ensemble) In the untargeted setting, GhostCert consistently generates larger spoofed radii than shadow baselines across all perturbation budgets. At $\sigma = 0.5$, GhostCert's spoofed radii approach or exceed the source radius (orange dashed line), indicating strongly certified defense bypass. At $\sigma = 1.0$, while all methods fall below the original ra-

dius due to stronger noise, GhostCert maintains a substantial advantage. In a targeted setting, in cases where there is significant ASR to report, GhostCert consistently generates larger spoofed radii than shadow baselines. In cases where the shadow variants generate similar spoofed radii, the ASR is negligibly low.

DoS Success. Interestingly, certification methods can abstain from making a decision. Failing to certify robustness for an input results in the verifier abstaining instead of making a potentially incorrect or vulnerable prediction. Table 2 reports abstain results observed in targeted attacks. When the given perturbation budget is inadequate for spoofing a certification (indicated by low ASR in Fig. 5), GhostCert input

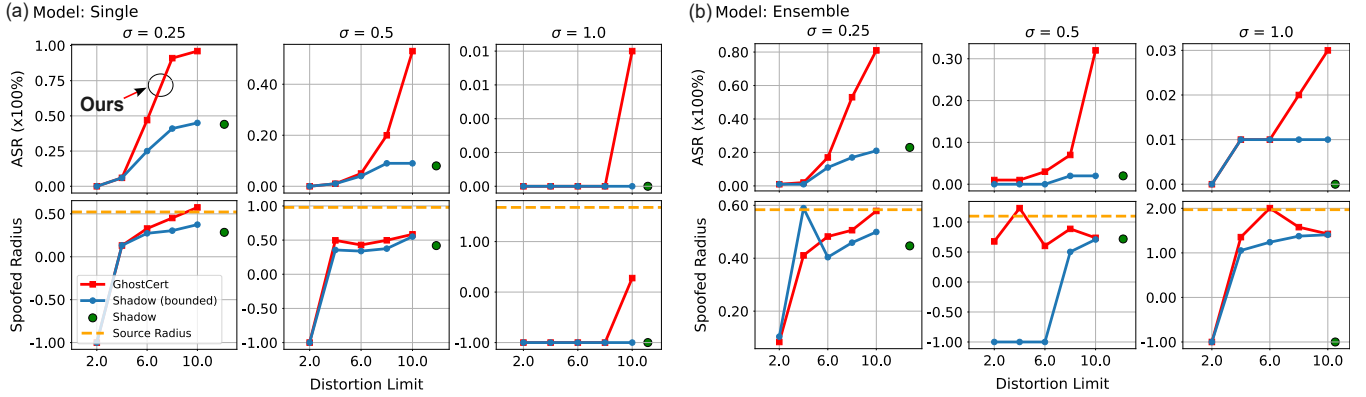


Figure 5: Comparing ASR and spoofed radii for three attacks in a *targeted* setting against (a) single ResNet-50 under Randomized Smoothing (RS) and (b) an ensemble of three consistency ResNet-50 models under RS vs. distortion $\|\delta\|_2$ budgets.

Table 2: DoS (Abstain) attack success (%) (Single).

$\ \delta\ _2$	Shadow (σ)			Shadow (Bounded) (σ)			GhostCert (σ)		
	0.25	0.5	1.0	0.25	0.5	1.0	0.25	0.5	1.0
2				14	8	9	8	84	8
4				31	18	18	20	68	12
6	25	27	34	25	29	23	16	52	21
8				24	29	35	4	38	34
10				21	38	39	2	45	45

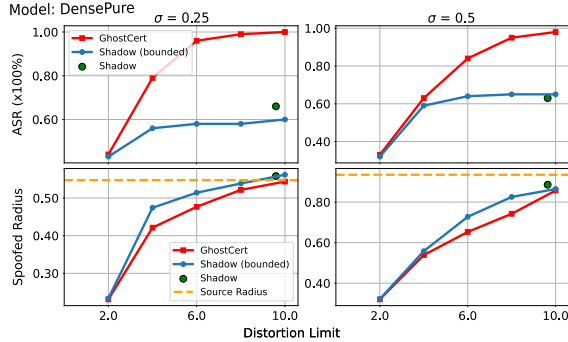


Figure 6: Comparing ASR and spoofed radii between three attacks in an *untargeted* setting against DensePure.

samples lead to a higher DoS success. Importantly, when the ASR for GhostCert is similar to Shadow Attack, the DoS success for our attack is generally higher than both shadow variants. This indicates the region-based perturbations are more effective but the adversarial crafted is near a decision boundary and the ϵ -bound is too large to spoof a certificate.

Attacking Denoised Smoothing (DensePure)

Attack Success Rate (ASR). GhostCert demonstrates superior and consistent performance across both noise levels as shown in Figure 6. At ($\sigma = 0.25$) GhostCert significantly outperforms shadow attacks and its variant across different perturbation budgets. GhostCert maintains 30 – 100% success rates while shadow method and its variant remain constrained at 30 – 65%. **Spoofed Radii.** Across perturbations budgets, GhostCert achieves spoofed certification radii that are slightly lower or comparable with Shadow Attack but

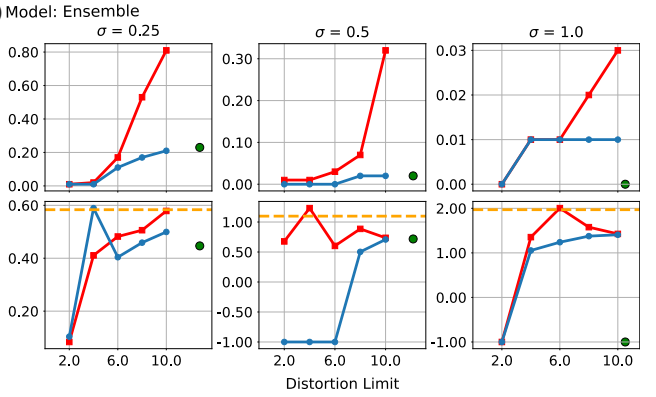


Figure 7: Naturalism/imperceptibility of the adversarial images generated by GhostCert vs. Shadow Attack across minimum & maximum distortion budgets. GhostCert images were consistently perceived as *more* natural looking.

consistently maintains a significantly higher ASR.

Evaluation of Imperceptibility: User Study

A user study compare the perceptual realism of adversarial images generated by GhostCert and Shadow Attack. For each distortion level ($\|\delta\|_2$), 10 successful image pairs (1 as control) were presented to workers on Amazon Mechanical Turk, with the display order of images from Shadow Attack and GhostCert randomized. To reduce noise, responses from workers who answered randomly or spent less than a minute on the task were excluded. The results from participants for each distortion level are shown in Figure 7. GhostCert consistently produced images rated as more natural across both high/low distortion levels.

Conclusion

We show region-based input manipulations preserve semantics while subtly shifting inputs to cause misclassification and yet receive large-radius certificates. Our method, GhostCert, outperforms the state-of-the-art Shadow Attack attack by achieving higher success in both misclassification and certificate spoofing, while producing more natural-looking, imperceptible adversarials. Our findings urge caution in using certification frameworks and encourage further research into certification methods and attack vectors.

Overview of Materials in the Appendices

We provide a brief overview of the set of additional experimental results and findings in the Appendices (Please see the extended version on <https://arxiv.org/>.)

1. A detailed analysis of our attack.
2. Details on metrics, hyper parameters and datasets.
3. Ablation studies assessing how various mask construction methods affect ASR in both targeted and untargeted attack scenarios.
4. Extended user study results comparing the adversarial images from GhostCert and the prior SoTA method Shadow Attack.
5. Investigating DoS success and attack success rate under targetted attack settings.

References

Athalye, A.; Carlini, N.; and Wagner, D. 2018. Obfuscated gradients give a false sense of security: Circumventing defenses to adversarial examples. In *International Conference on Machine Learning (ICML)*.

Bhattad, A.; Chong, M. J.; Liang, K.; Li, B.; and Forsyth, D. A. 2020. Unrestricted Adversarial Examples via Semantic Manipulation. In *International Conference on Learning Representations*.

Biggio, B.; Corona, I.; Maiorca, D.; Nelson, B.; Šrndić, N.; Laskov, P.; Giacinto, G.; and Roli, F. 2013. Evasion Attacks against Machine Learning at Test Time. In Blockeel, H.; Kersting, K.; Nijssen, S.; and Železný, F., eds., *Machine Learning and Knowledge Discovery in Databases*, 387–402. Berlin, Heidelberg: Springer Berlin Heidelberg. ISBN 978-3-642-40994-3.

Brendel, W.; Rauber, J.; and Bethge, M. 2018. Decision-based adversarial attacks: Reliable attacks against black-box machine learning models. In *International Conference on Learning Recognitions (ICLR)*.

Buckman, J.; Roy, A.; Raffel, C.; and Goodfellow, I. 2018. Thermometer Encoding: One Hot Way To Resist Adversarial Examples. In *International Conference on Learning Representations*.

Carlini, N.; Tramèr, F.; Dvijotham, K. D.; and Kolter, J. Z. 2023. (Certified!!) Adversarial Robustness for Free!

Carlini, N.; and Wagner, D. 2017a. Adversarial Examples Are Not Easily Detected: Bypassing Ten Detection Methods. *arXiv:1705.07263*.

Carlini, N.; and Wagner, D. 2017b. Towards evaluating the robustness of neural networks. In *IEEE Symposium on Security and Privacy (SSP)*.

Cohen, J. M.; Rosenfeld, E.; and Kolter, J. Z. 2019. Certified Adversarial Robustness via Randomized Smoothing. *arXiv preprint arXiv:1902.02918*.

Croce, F.; and Hein, M. 2020. Reliable evaluation of adversarial robustness with an ensemble of diverse parameter-free attacks.

Dalvi, N.; Domingos, P.; Mausam; Sanghai, S.; and Verma, D. 2004. Adversarial classification. In *Proceedings of the Tenth ACM SIGKDD International Conference on Knowledge Discovery and Data Mining*, KDD '04, 99–108. New York, NY, USA: Association for Computing Machinery. ISBN 1581138881.

Deng, J.; Dong, W.; Socher, R.; Li, L.; Li, K.; and Fei-Fei, L. 2009a. ImageNet: A large-scale hierarchical image database. In *Computer Vision and Pattern Recognition (CVPR)*.

Deng, J.; Dong, W.; Socher, R.; Li, L.-J.; Li, K.; and Fei-Fei, L. 2009b. ImageNet: A large-scale hierarchical image database. In *2009 IEEE Conference on Computer Vision and Pattern Recognition*, 248–255.

Doan, B. G.; Abbasnejad, E. M.; Shi, J. Q.; and Ranasinghe, D. C. 2022. Bayesian Learning with Information Gain Provably Bounds Risk for a Robust Adversarial Defense. In *International Conference on Machine Learning (ICML)*.

Ghiasi, A.; Shafahi, A.; and Goldstein, T. 2020. Breaking Certified Defenses: Semantic Adversarial Examples With Spoofed Robustness Certificates. In *International Conference on Learning Representations*.

Goodfellow, I. J.; Shlens, J.; and Szegedy, C. 2015. Explaining and Harnessing Adversarial Examples.

Guo, C.; Rana, M.; Cisse, M.; and van der Maaten, L. 2018. Countering Adversarial Images using Input Transformations. In *International Conference on Learning Representations*.

Hayes, J. 2020. Extensions and limitations of randomized smoothing for robustness guarantees. *arXiv:2006.04208*.

Horváth, M. Z.; Mueller, M. N.; Fischer, M.; and Vechev, M. 2022. Boosting Randomized Smoothing with Variance Reduced Classifiers. In *International Conference on Learning Representations*.

Jeong, J.; and Shin, J. 2020. Consistency Regularization for Certified Robustness of Smoothed Classifiers. In *Advances in Neural Information Processing Systems*.

Kirillov, A.; Mintun, E.; Ravi, N.; Mao, H.; Rolland, C.; Gustafson, L.; Xiao, T.; Whitehead, S.; Berg, A. C.; Lo, W.-Y.; et al. 2023. Segment anything. In *Proceedings of the IEEE/CVF International Conference on Computer Vision*, 4015–4026.

Kurakin, A.; Goodfellow, I. J.; and Bengio, S. 2017. Adversarial examples in the physical world.

Lecuyer, M.; Atlidakis, V.; Geambasu, R.; Hsu, D.; and Jana, S. 2019. Certified Robustness to Adversarial Examples with Differential Privacy. *arXiv:1802.03471*.

Levine, A.; and Feizi, S. 2020. Wasserstein Smoothing: Certified Robustness against Wasserstein Adversarial Attacks. In *Proceedings of the Twenty Third International Conference on Artificial Intelligence and Statistics*.

Li, L.; Xie, T.; and Li, B. 2023. SoK: Certified Robustness for Deep Neural Networks . In *2023 IEEE Symposium on Security and Privacy (SP)*.

Lyu, Z.; Ko, C.; Kong, Z.; Wong, N.; Lin, D.; and Daniel, L. 2020. Fastened CROWN: Tightened Neural Network Robustness Certificates. In *The Thirty-Fourth AAAI Conference on Artificial Intelligence*.

Madry, A.; Makelov, A.; Schmidt, L.; Tsipras, D.; and Vladu, A. 2018. Towards deep learning models resistant to adversarial attacks. In *International Conference on Learning Recognitions (ICLR)*.

Papernot, N.; McDaniel, P.; Goodfellow, I.; Jha, S.; Celik, Z. B.; and Swami, A. 2017. Practical Black-Box Attacks against Machine Learning. In *ACM Asia Conference on Computer and Communications Security (ASIA CCS)*.

Papernot, N.; McDaniel, P.; Wu, X.; Jha, S.; and Swami, A. 2016. Distillation as a Defense to Adversarial Perturbations Against Deep Neural Networks. In *2016 IEEE Symposium on Security and Privacy (SP)*, 582–597.

Rebuffi, S.-A.; Gowal, S.; Calian, D. A.; Stimberg, F.; Wiles, O.; and Mann, T. 2021. Fixing Data Augmentation to Improve Adversarial Robustness. arXiv:2103.01946.

Salman, H.; Li, J.; Razenshteyn, I.; Zhang, P.; Zhang, H.; Bubeck, S.; and Yang, G. 2019. Provably robust deep learning via adversarially trained smoothed classifiers. In *Advances in Neural Information Processing Systems*.

Salman, H.; Yang, J. L.; Zhang, H.; Zhang, H.; Hsieh, C.-J.; and Madry, A. 2020. Denoised Smoothing: A Provable Defense for Pretrained Classifiers. In *Advances in Neural Information Processing Systems (NeurIPS)*.

Samangouei, P.; Kabkab, M.; and Chellappa, R. 2018. Defense-GAN: Protecting Classifiers Against Adversarial Attacks Using Generative Models. In *International Conference on Learning Representations*.

Selvaraju, R. R.; Cogswell, M.; Das, A.; Vedantam, R.; Parikh, D.; and Batra, D. 2017. Grad-CAM: Visual Explanations from Deep Networks via Gradient-based Localization. In *Proceedings of the IEEE International Conference on Computer Vision (ICCV)*, 618–626.

Shafahi, A.; Najibi, M.; Ghiasi, A.; Xu, Z.; Dickerson, J.; Studer, C.; Davis, L. S.; Taylor, G.; and Goldstein, T. 2019. Adversarial Training for Free! In *Proceedings of the 33rd International Conference on Neural Information Processing Systems (NeurIPS)*.

Shahin Shamsabadi, A.; Sanchez-Matilla, R.; and Cavallaro, A. 2020. ColorFool: Semantic Adversarial Colorization. In *2020 IEEE/CVF Conference on Computer Vision and Pattern Recognition (CVPR)*.

Szegedy, C.; Zaremba, W.; Sutskever, I.; Bruna, J.; Erhan, D.; Goodfellow, I.; and Fergus, R. 2014. Intriguing properties of neural networks. In *International Conference on Learning Recognitions (ICLR)*.

Tramer, F.; Carlini, N.; Brendel, W.; and Madry, A. 2020. On adaptive attacks to adversarial example defenses. In *Advances in Neural Information Processing Systems*.

Vo, V. Q.; Abbasnejad, E.; and Ranasinghe, D. C. 2022. RamBoAttack: A Robust Query Efficient Deep Neural Network Decision Exploit. In *Proceedings of the 2022 Network and Distributed System Security Symposium (NDSS)*.

Weng, T.-W.; Zhang, H.; Chen, H.; Song, Z.; Hsieh, C.-J.; Boning, D.; Dhillon, I. S.; and Daniel, L. 2018. Towards Fast Computation of Certified Robustness for ReLU Networks. arXiv:1804.09699.

Wong, E.; Rice, L.; and Kolter, J. Z. 2020. Fast is better than free: Revisiting adversarial training. arXiv:2001.03994.

Xiao, C.; Chen, Z.; Jin, K.; Wang, J.; Nie, W.; Liu, M.; Anandkumar, A.; Li, B.; and Song, D. 2023. DensePure: Understanding Diffusion Models towards Adversarial Robustness.

Zhang, H.; Chen, H.; Xiao, C.; Li, B.; Boning, D.; and Hsieh, C.-J. 2019. Towards Stable and Efficient Training of Verifiably Robust Neural Networks.

Zhang, J.; Chen, Z.; Zhang, H.; Xiao, C.; and Li, B. 2023. DiffSmooth: Certifiably Robust Learning via Diffusion Models and Local Smoothing. arXiv:2308.14333.

Attack Analysis

In this section, we first articulate the novelty of the proposed attack and delineate its fundamental distinctions from conventional approaches—e.g., PGD (Madry et al. 2018), Wasserstein (Levine and Feizi 2020), and semantic attacks (Shahin Shamsabadi, Sanchez-Matilla, and Cavallaro 2020; Bhattad et al. 2020)—with particular emphasis on differences in the threat model and optimization objective. We subsequently analyze the effectiveness of the proposed method compare to Shadow Attack.

A new threat model. Standard attacks (including ℓ_p -, Wasserstein- and semantic-based methods) are designed to induce misclassification of the base classifier f while keeping perturbations imperceptible. Our goal is strictly harder: we target certified defenses—*randomized smoothing*—and aim to produce inputs that are misclassified by the smoothed classifier g and simultaneously receive a large, yet spurious, certified radius (not just the base classifier f). Attacking a certifier requires controlling the classifier’s behavior across a neighborhood of noisy samples, not just at a single point.

New objective. PGD is designed to force misclassification of the base classifier. Our objective is to simultaneously induce misclassification and manipulate the randomized-smoothing certifier, producing adversarial inputs that are both incorrect and receive a (spoofed) robustness certificate. To achieve this goal, we have to maximize sample agreement under the smoothing distribution rather than a single sample. This is reflected in the certification-aware losses and constraints in equation 6, 7 and 8. Further, in the targeted setting we investigate, we observe a potential new threat surface, Denial of Service attacks, against certified models not explored in Shadow Attack.

Attack Effectiveness and comparison with Shadow Attack. The Shadow Attack focuses on generating visually natural and smooth perturbations by regularizing pixel-level changes through total variation and other constraints rather than imperceptibility. Its optimization goal is to ensure perturbations look natural, while still crossing the classifier’s decision boundary. Thus, it turns semantic constraints into regularizers and adds them to the attack loss. This creates

a multi-objective optimization where the optimizer must trade off attack strength against perceptual/semantic penalties, which can make it difficult to find low-distortion solutions that also satisfy certification criteria. We take another approach to maintain natural-looking but still achieve low distortion by formulating the problem as a constrained optimization. We restrict the perturbation in a salient and natural object bounded area by using semantic segmentation and GradCAM-derived masks. This reduces the search space and focuses the optimization on semantically coherent regions. Therefore, it improves the effectiveness of our attack and achieve significantly low distortion.

Task Definitions and Experiment Setup

Metrics. We provide more formal descriptions of the metrics used in our evaluations below for completeness.

- **Attack Success Rate (Untargeted settings):** We follow the definition in Shadow Attack and ASR is calculated by

$$\left\{ \frac{\#\text{of samples not certified as source label}}{\text{Total number of attack samples}} \right\}.$$

- **Attack Success Rate (Targeted settings):** This defines the success rate of spoofing a certificate targeted attack. We defined the metric as follows:

$$\left\{ \frac{\#\text{of samples certified as the target class}}{\text{Total number of attack samples}} \right\}.$$

- **Denial of Service (DoS)/Abstain Success Rate (Targeted settings):** We defined the metric as follows:

$$\left\{ \frac{\#\text{of samples resulting in an abstain decision}}{\text{Total number of attack samples}} \right\}.$$

- **Score:** Used to measure naturalism/imperceptibility with human annotators by counting votes as follows:

$$\left\{ \frac{\#\text{times GhostCert image is selected}}{\text{The total number of human annotator participants}} \right\}.$$

We expect scores to be higher for GhostCert as the perturbations are less perceptible and more annotators in Amazon Mechanical Turk (AMT) agree with the same answer.

Dataset. We employed ImageNet (ILSVRC2012), which is a subset of the ImageNet dataset specifically used for the ImageNet Large Scale Visual Recognition Challenge in 2012 containing over 1.2 million images distributed across 1,000 different classes.

Hyper-Parameters. Detailed information about the hyper-parameters used can be found in Table 3.

Ablation Study

We conducted several ablation studies to examine how different mask construction strategies influence ASR under both targeted and untargeted attack settings. Specifically, we evaluated:

Table 3: Hyper-parameters setting in our experiments.

Name	Value	Notes
σ	0.25, 0.5 and 1.0	Standard deviations of isotropic gaussian noise
$\ \delta\ _2$	2, 4, 6, 8, 10	Maximum distortion budgets for perturbation
λ	0.0001	The step size for gradient descent
α	0.001	Failure probability in Randomized Smoothing
N_0	10	The number of Monte Carlo samples to use for selection
N	1000	The number of Monte Carlo samples to use for estimation
k	5	The number of masks used to generate the final mask after saliency analysis

Defense	ϵ	Attack	ASR (Random)	ASR (Ours)
Ensemble ($\sigma = 0.5$)	2	Untargeted	33.33	35
	10		90	90
	2	Targeted	0	0
	10		5	30

Table 4: ASR comparison between region-based and saliency guided perturbations—GhostCert—and a 50% random region baseline for 20 images from our ImageNet test set.

- A comparison between our saliency-guided region selection approach and a random-region baseline, where each pixel is independently selected with 50% probability. The results, shown in Table 4 show that our method achieves higher ASR, particularly under the harder, targeted attacks.
- A comparison between our saliency-guided region selection and using k randomly chosen regions (without saliency). In both cases, k is set to 5 since we selected the top 5 in our approach. The distinction is in region selection: our method selects the top k regions from segmentation based on saliency ranking, while the comparison baseline selects k regions uniformly at random. As shown in Table 5, ours consistently achieves higher ASR in both targeted and untargeted settings.
- The sensitivity of ASR with respect to the choice of k —which determines the number of regions, ranked by saliency, aggregated to construct the region for perturbation or the *salient region*. As shown in Table 6, when $k = 3$, the ASR is lower in both targeted and untargeted settings. Setting k to 5 or 7 leads to similar ASR across both targeted and untargeted settings. In our approach, we chose the top 5 masks from SAM based on saliency analysis.

User study

We conducted a user study to evaluate the perceptual realism of adversarial images generated by GhostCert and Shadow Attack. For each distortion level ($\|\delta\|_2$), 10 successful adversarial image pairs were shown to human annotators on Amazon Mechanical Turk (AMT), with the image order between Shadow Attack and GhostCert randomized to remove bias. To ensure high-quality responses, participants who answered randomly or completed the task in under a minute were excluded. We determined random answers by placing an image among the 10 with very obvious deviations and manipulation in the set. Subsequently we used responses

Defense	ϵ	Attack	Region Proposals only	Region Proposals + Saliency (ours)
Ensemble $(\sigma = 0.5)$	2	Untargeted	10	35
	10		45	90
	2	Targeted	0	0
	10		0	30

Table 5: ASR comparison between region-based and saliency guided perturbations (ours) and k random regions (binary segmentation masks or region proposals produced and selected without saliency guiding). Our method selects the top $k = 5$ region proposals ranked by saliency, while the baseline selects $k = 5$ random regions. Results show higher ASR for our method in both (targeted and untargeted) attack settings for 20 images from our ImageNet test set.

Defense	ϵ	Attack	ASR, $k = 3$	ASR, $k = 5$	ASR, $k = 7$
Ensemble $(\sigma = 0.5)$	2	Untargeted	25	35	30
	10		90	90	90
	2	Targeted	0	0	0
	10		15	30	35

Table 6: Sensitivity Analysis. ASR achieved with difference choice of k used to generated the salient region (see Figure 1). Using $k = 3$ results in noticeably lower ASR for both targeted and untargeted attacks, whereas $k = 5$ and $k = 7$ yield comparable performance. We used $k = 5$ for all our evaluations.

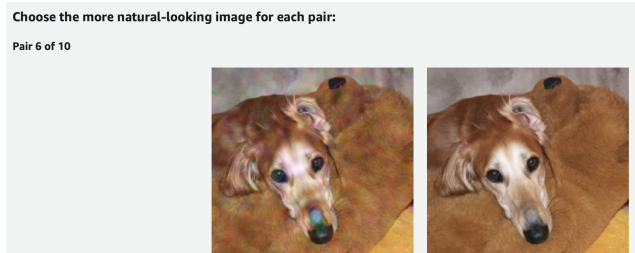
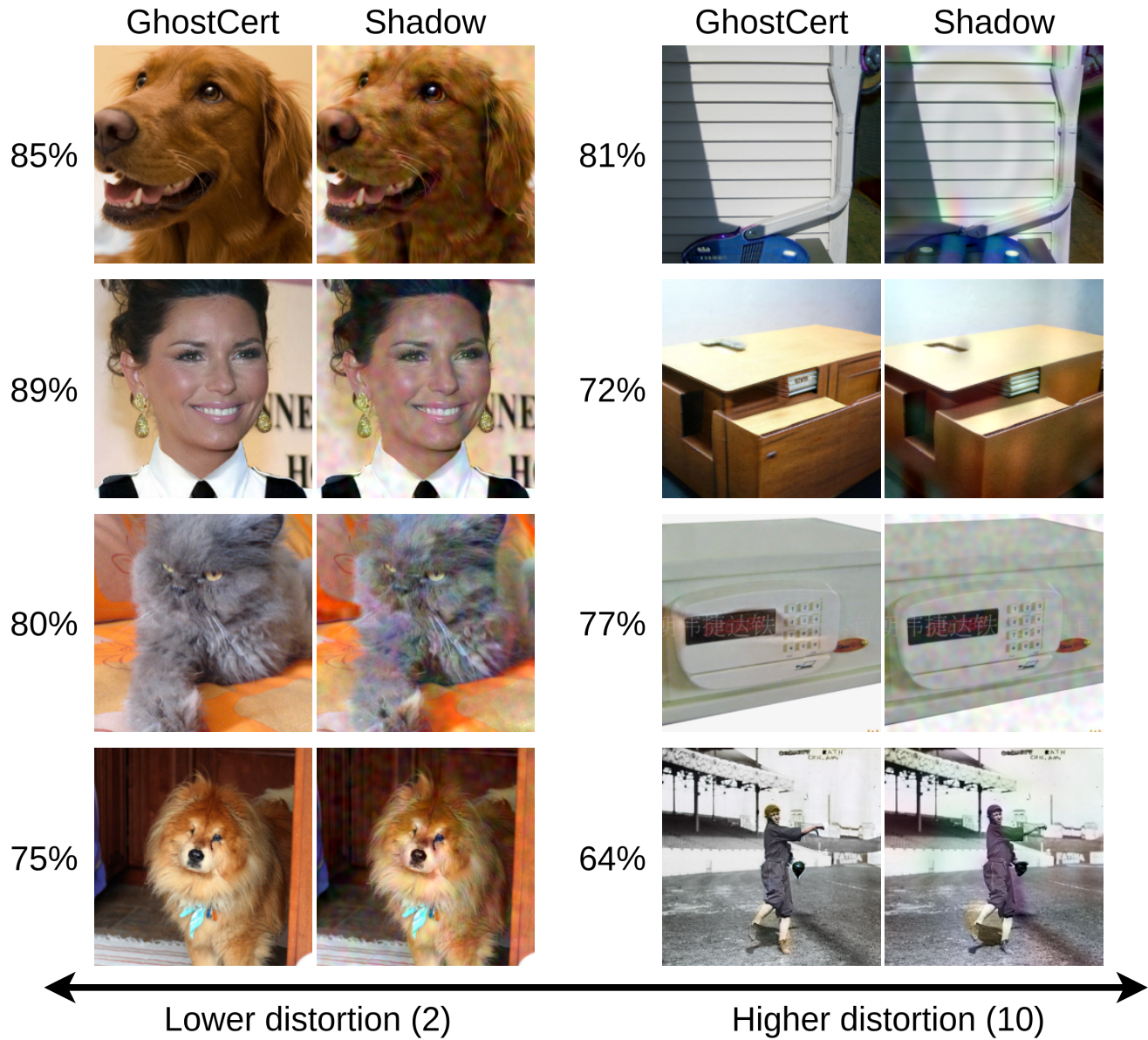


Figure 8: The UI presented to AMT annotators. Once an option is chosen, the users are presented with the next image pair.

to the pair with this test image to remove responses that were unreliable.

The study interface was paginated, preventing users from anticipating upcoming images. Figure 8 shows the UI that is presented to an annotator in AMT. Figure 9 shows results from nearly 50 valid participants for distortion levels 2 and 10, revealing that GhostCert consistently produced images perceived as more natural across both low and high distortion levels.



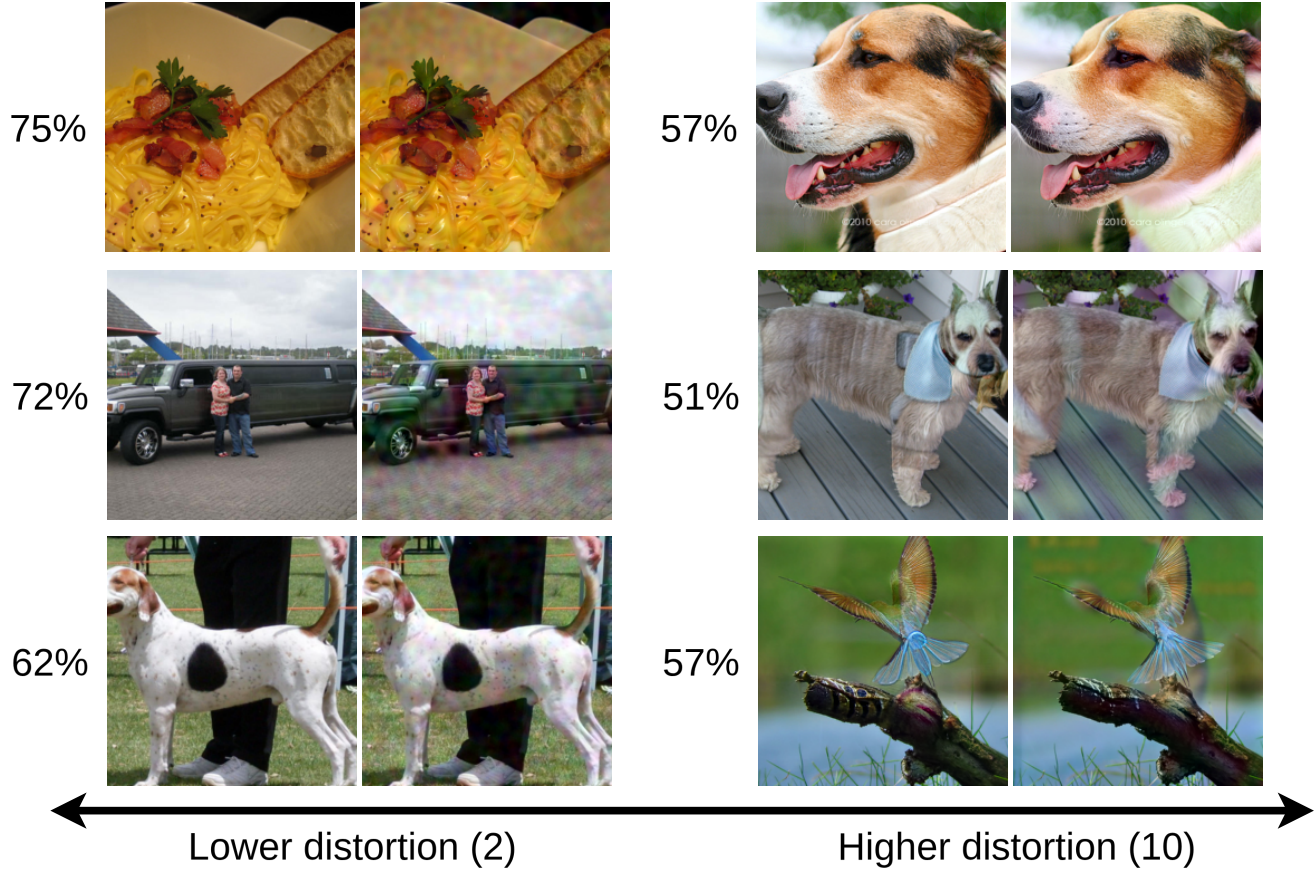


Figure 9: Naturalism (imperceptibility) of adversarial images generated by GhostCert and Shadow Attack across minimum and maximum distortion levels. Images produced by GhostCert were consistently rated as more natural. At a higher distortion level ($\|\delta\|_2 = 10$), as expected, the difference in perceived naturalness was less pronounced, although GhostCert images were still considered to be more natural looking.

Investigating DoS Success and Attack Success Rate

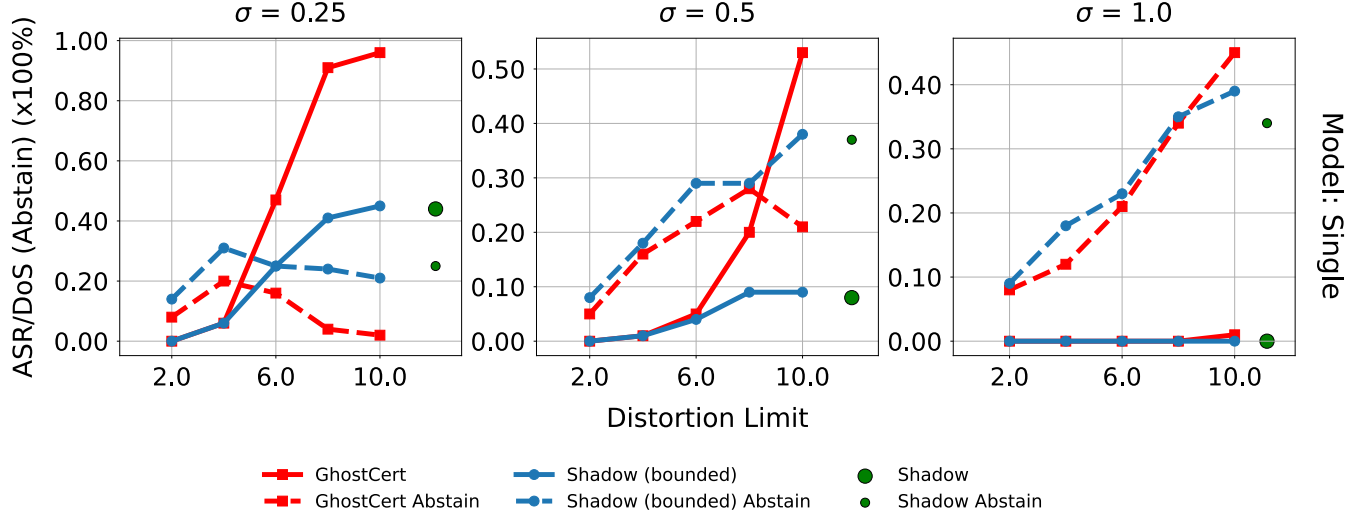


Figure 10: Comparing of DoS (abstain) and ASR (misclassified with the verifier issuing a certification radius) between three attacks in a targeted setting against a Single model (ResNet-50) under RS. As expected when ASR is high, the DoS rate is low, while ASR of GhostCert is higher, generating spoofed certificates under a budget of 10 is hard for both methods for model trained with $\sigma = 1.0$.

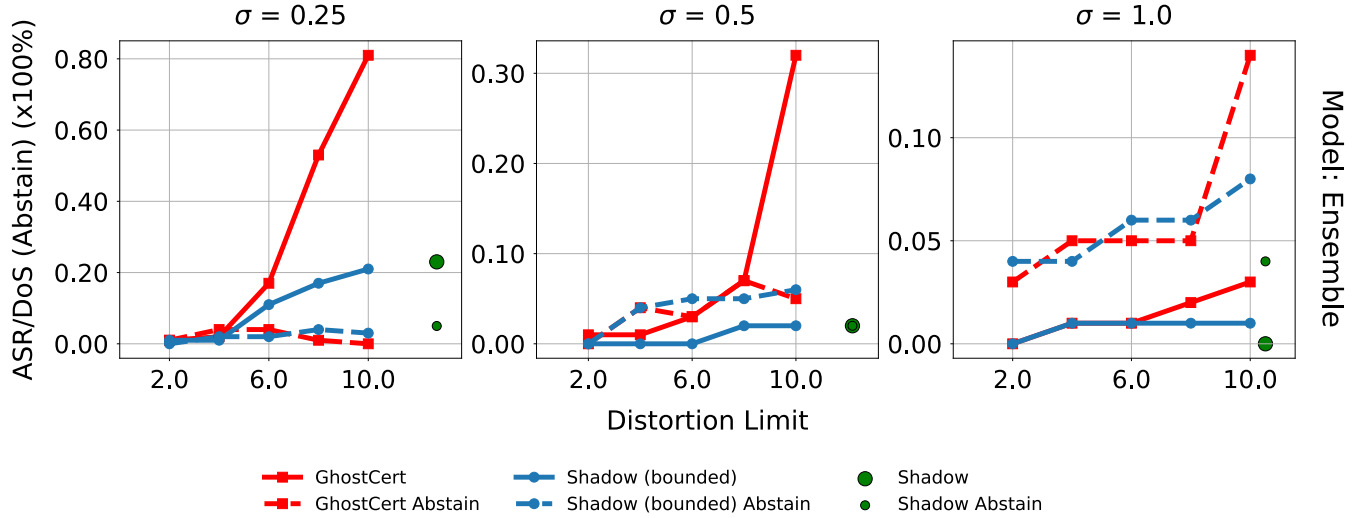


Figure 11: Comparing of DoS (abstain) and ASR (misclassified with the verifier issuing a certification radius) between three attacks in a targeted setting against an ensemble of three consistency ResNet-50 models under RS. As expected when ASR is high, the DoS rate is low, while ASR of GhostCert is higher, generating spoofed certificates under a budget of 10 is is increasingly harder for both methods for model trained with $\sigma = 0.5$ and 1.0 . Interestingly, GhostCert is observed to produce more effective adversarial against more robust models as the DoS success is higher against the $\sigma = 0.1$ ensembler under RS.